A New Method of QPSK Demodulation Based on Modified 26 GHz Six-Port Circuit

Lotfi Osman, Imen Sfar, and Ali Gharsallah

Department of Physics, UR "CSEHF" - 05/UR/11-10
University of Sciences El Manar, 2092 Tunisia
lotfi.osman@supcom.rnu.tn, imen.sfar@voila.fr, ali.gharsallah@gmail.com

Abstract - In this paper, we propose to study a new demodulation technique of a QPSK signal exploited in a homodyne receiver by using a modified six-port circuit as demodulator. We will present two techniques of the same structure but we will retain only the best configuration. The new approach allows the integration of the receiver module in a high-performance millimeter wave technology, reducing the size and overall cost of the receivers. This approach is validated by using Agilent's Advanced Design System (ADS) software for RF design and simulation.

Index Terms - ADS software, direct conversion receiver, QPSK demodulator, Six-port circuit.

I. INTRODUCTION

Due to the overwhelming demand for wireless communications, efforts were deployed to simplify the structure of receivers used in demodulators thus reducing both their dimensions and costs. The new communication systems need a high fidelity transmission of high-speed information. In the case of conventional receivers, the manufacturing defaults which are unavoidable in high-frequency generate distortions of the in-phase and quadrature RF signals. We know that the increase in frequency leads to a decrease in wavelength. It then becomes more and more difficult to perform couplers with excellent performance [1]. The new architecture shown in Fig. 1 makes it possible through a new phase demodulation system not only to correct the imperfections of manufacture, but also to adjust both the gain and phase errors of conventional demodulators. The six-port structure was successfully used in the design of network analyzers and other applications. Recall that the theory of the six-port circuit was widely developed by many researchers in order to show its qualities as a reflectometer [2, 3].

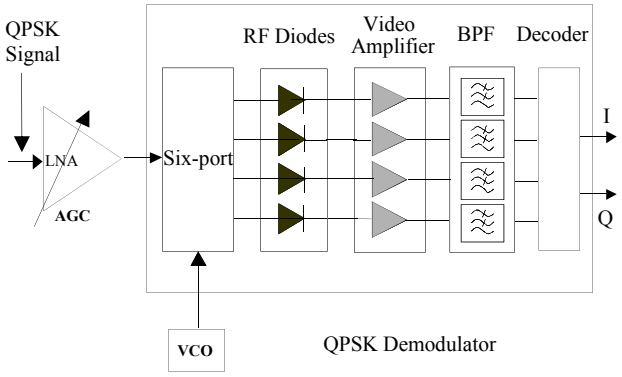

Fig. 1. Structure of the new QPSK demodulation technique.

The circuit can be considered as a black box with two inputs, one for the reference signal and the other for the signal to identify, with four possible combinations between the input signals.

In this paper, we propose a new technique to extract the information contained in a quadrature modulated signal. This will be achieved with a new type of QPSK demodulator based on a modified six-port circuit. But first of all, we will explain how a conventional six-port junction was initially designed to measure the reflection coefficient of a load (one-port device).

II. THE CONVENTIONAL SIX-PORT JUNCTION

It is a linear passive component composed of several couplers connected by transmission lines [4, 5]. It was originally designed in the sixties to measure the phase of RF signals. This component has two inputs and four outputs. The first input is

Submitted On: Dec. 7, 2011
Accepted On: May 22, 2012

reserved to the reference signal; whereas, the second input receives the signal to be identified. The six-port structure has been successfully used in the design of network analyzers and other similar applications. The theory of the six-port junction was further developed by Glenn F. Engen [6] by highlighting its qualities of reflectometer.

The response of this junction can be characterized by the following set of equations that express the powers at its four outputs:

$$\begin{cases} P_1 = |b_1|^2 = |\mathrm{Aa} + \mathrm{Bb}|^2 \\ P_2 = |b_2|^2 = |\mathrm{Ca} + \mathrm{Db}|^2 \\ P_3 = |b_3|^2 = |\mathrm{Ea} + \mathrm{Fb}|^2 \\ P_4 = |b_4|^2 = |\mathrm{Ga} + \mathrm{Hb}|^2 \end{cases}, \quad (1)$$

where the coefficients A to H are complex constants which must be determined by a calibration procedure, and a & b are incident and reflected waves at the input of a load.

Figure 2 illustrates a schema of a six-port reflectometer using 90° hybrid couplers to measure the reflection coefficient Γ of the load.

The schema of a 90° hybrid coupler and its scattering matrix are shown in Fig. 3.

(a)

$$S = \frac{1}{\sqrt{2}}\begin{bmatrix} 0 & \mathrm{j} & 1 & 0 \\ \mathrm{j} & 0 & 0 & 1 \\ 1 & 0 & 0 & \mathrm{j} \\ 0 & 1 & \mathrm{j} & 0 \end{bmatrix}. \quad (2)$$

(b)

Fig. 3. (a) 90° hybrid coupler; (b) corresponding scattering matrix.

The following set of equations give the expressions of powers at the four outputs:

$$\begin{cases} P_1 = \frac{|a|^2}{4}|\Gamma - 1|^2 \\ P_2 = \frac{|a|^2}{8}|\Gamma - (-1 + \mathrm{j})|^2 \\ P_3 = \frac{|a|^2}{8}|\Gamma - (-1 - \mathrm{j})|^2 \\ P_4 = \frac{|a|^2}{4} \end{cases}. \quad (3)$$

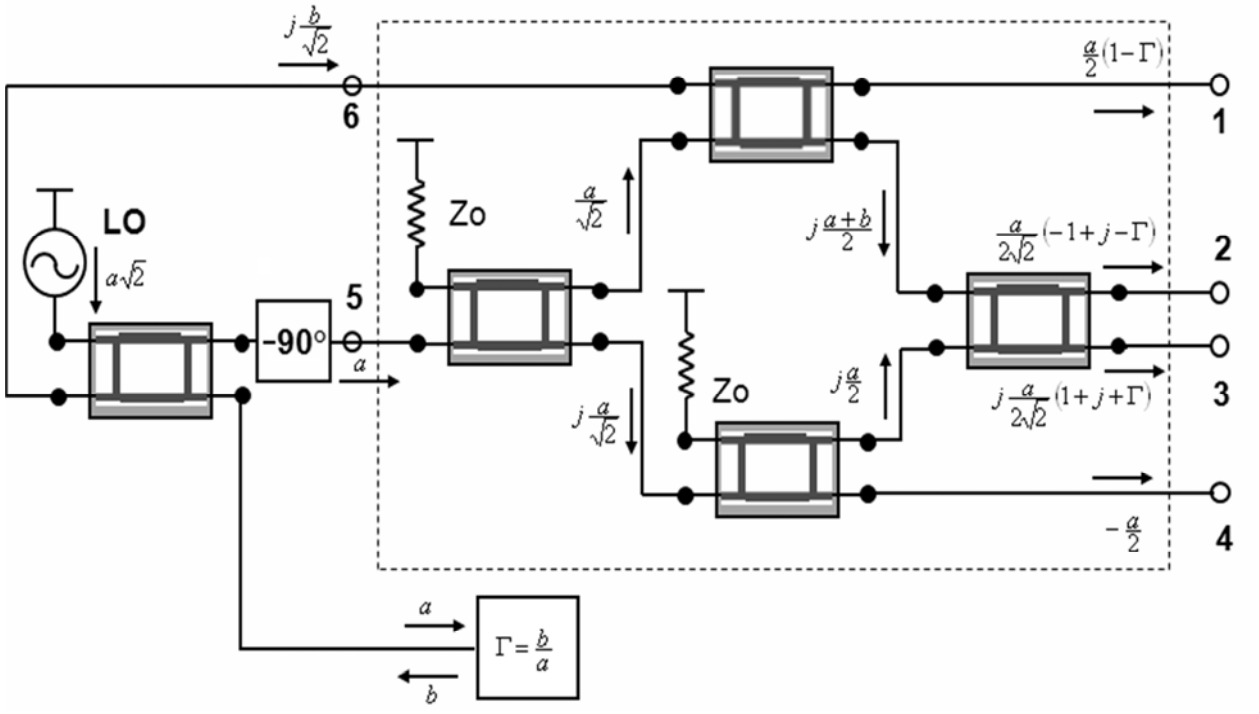

Fig. 2. Block diagram of the conventional six-port junction.

Only P_4 is independent of Γ. It will therefore be used as reference power, which leads to the following three normalized powers:

$$\begin{cases} p_1 = \dfrac{P_1}{P_4} = |\Gamma - 1|^2 \Rightarrow |\Gamma - 1| = \sqrt{p_1} \\ p_2 = \dfrac{P_2}{P_4} = |\Gamma - (-1 + \mathrm{j})|^2 \Rightarrow \\ \qquad |\Gamma - (-1 + \mathrm{j})| = \sqrt{2p_2} \\ p_3 = \dfrac{P_3}{P_4} = |\Gamma - (-1 - \mathrm{j})|^2 \Rightarrow \\ \qquad |\Gamma - (-1 - \mathrm{j})| = \sqrt{2p_3} \end{cases} . \quad (4)$$

The three resulting equations are the equations of three circles whose centers are:

$$q_1 = 1,\ q_2 = -1 + j \text{ and } q_3 = -1 - j.$$

Figure 4 shows the graphical representation of these three circles.

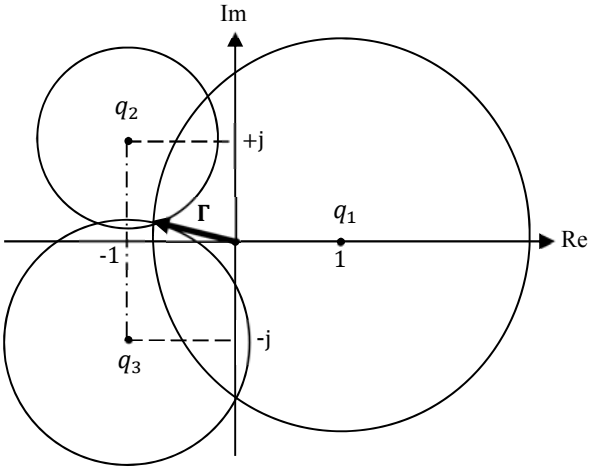

Fig. 4. Graphical representation of the reflection coefficient Γ.

The intersection point of these three circles will give us the value of the reflection coefficient Γ at the input of the device. The position of the points q_i depends on the architecture of the six-port junction and, ideally, the three points should be located at 120° from each other and equidistant from the center.

Finally, the measurement of the reflection coefficient Γ consists in determining the power levels at the four output ports and developing a suitable algorithm by considering one of the output ports as reference.

III. PRINCIPLE OF A MODIFIED SIX-PORT CIRCUIT

The modified six-port circuit is performed with two types of couplers: Wilkinson coupler acts as a power splitter [7, 8] and a 90° hybrid coupler produces two output signals phase shifted by 90°. We first represent in Fig. 5 below, the scheme of a Wilkinson coupler and its scattering matrix.

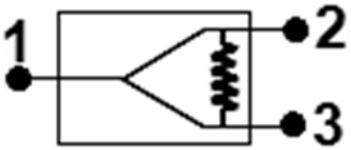

(a)

$$S = -\frac{\mathrm{j}}{\sqrt{2}}\begin{bmatrix} 0 & 1 & 1 \\ 1 & 0 & 1 \\ 1 & 1 & 0 \end{bmatrix}. \quad (5)$$

(b)

Fig. 5. (a) Wilkinson coupler; (b) corresponding scattering matrix.

Figure 6 shows the modified six-port circuit with its two inputs (a_5 & a_6) and four outputs. Assuming that the input signals have the same amplitude and that each port is matched, the wave equations to those inputs and outputs ports can be expressed as follows:

$$\begin{cases} a_5 = a\exp(j\theta_5) \\ a_6 = a\exp(j\theta_6) \\ b_1 = -j\dfrac{a}{2}\exp(j\theta_5).\{1 - \exp[j(\theta_6 - \theta_5)]\} \\ b_2 = \dfrac{a}{2}\exp(j\theta_5)\left\{1 - \exp\left[j\left(\theta_6 - \theta_5 - \dfrac{\pi}{2}\right)\right]\right\} \\ b_3 = \dfrac{a}{2}\exp(j\theta_5).\{1 - \exp[j(\theta_6 - \theta_5 - \pi]\} \\ b_4 = -j\dfrac{a}{2}\exp(j\theta_5)\left\{1 - \exp\left[j\left(\theta_6 - \theta_5 + \dfrac{\pi}{2}\right)\right]\right\} \end{cases} . \quad (6)$$

Given that the output power of a matched load is equal to $|b|^2$, we can notice that for each output there is a phase shift Δθ equal to (θ_6 - θ_5) between the 2 input signals corresponding to a zero power. By using the circuit as a QPSK demodulator, we can differentiate four modulation states by using output power measurements and detecting that which it is minimal with regard to the others [9].

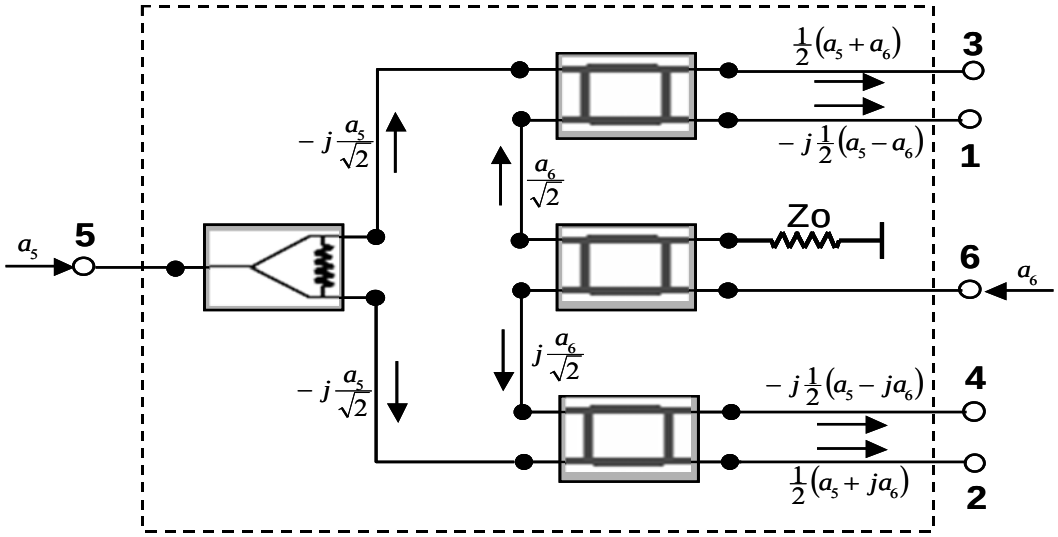

Fig. 6. Block diagram of the modified six-port.

IV. STUDY OF A NEW SIX-PORT STRUCTURE

Having as basic structure the diagram of the modified six-port junction represented in Fig. 6, we designed this structure by considering two different architectures for the hybrid couplers. The circuit is simulated at 26 GHz center frequency with Momentum 3D Planar EM Simulator of Advanced Design System software [10] by using microstrip lines. The parameters of the used substrate are: 0.254 mm for the thickness and 9.9 for the relative permittivity.

Figures 7 and 8 show two structures of the six-port circuit performed with square and round hybrid couplers, respectively.

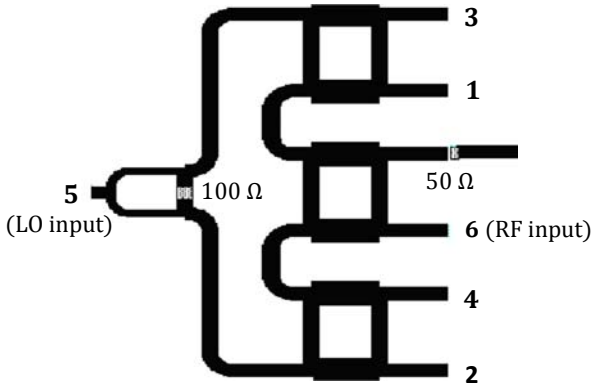

Fig. 7. Six-port performed with square hybrid couplers.

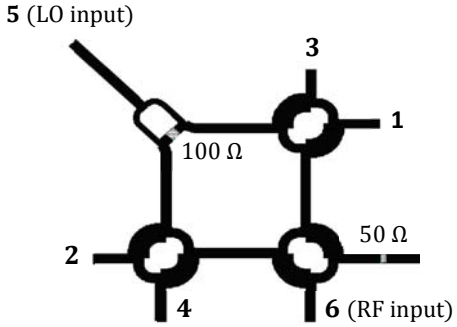

Fig. 8. Six-port performed with round hybrid couplers.

We present hereafter the simulation results of Scattering parameters (S-parameters) of both structures in a frequency band around 26 GHz.

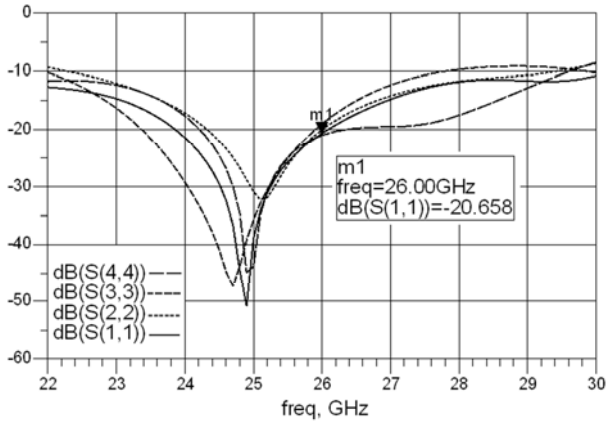

Fig. 9. Output reflection coefficients of the structure with square hybrid couplers.

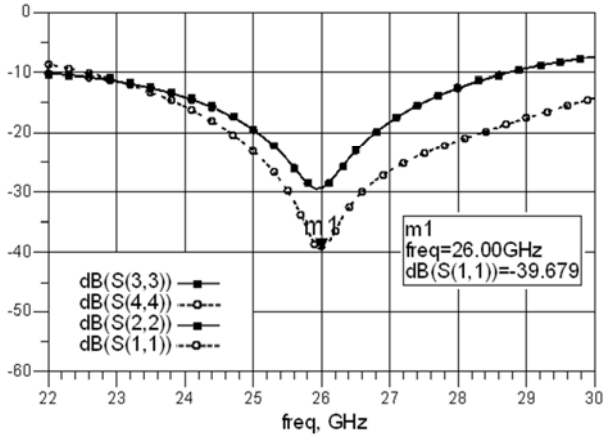

Fig. 10. Output reflection coefficients of the structure with round hybrid couplers.

Figures 9 and 10 show the matching values at their output ports in [22-30] GHz frequency band.

As can be seen, we get a better matching at f = 26 GHz for the structure based on round hybrid couplers with $S_{11} = S_{44} \approx$ -39 dB and $S_{22} = S_{33} \approx$ -30 dB. It follows that the round shapes of couplers used in this structure contributes to this good matching compared to that based on square hybrid couplers with $S_{ii} \approx$ -20 dB at 26 GHz for i = 1 to 4.

That is why we present in what follows results of the phase and the coupling obtained only from the structure with round hybrid couplers. Figures 11 and 12 show the transmission curves S_{5i} and S_{6i} with i = 1 to 4. All values obtained at f = 26 GHz are close to - 6 dB ($= -20\log\frac{1}{2}$).

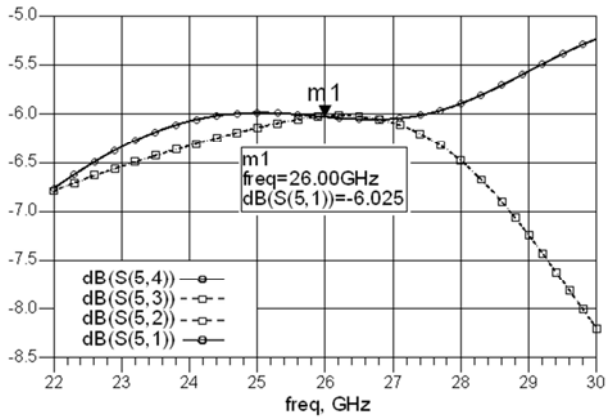

Fig. 11. Transmission coefficients between LO input port (N°5) and output ports.

The transmission phases between each two output ports are represented in Fig. 13 (a) and (b).

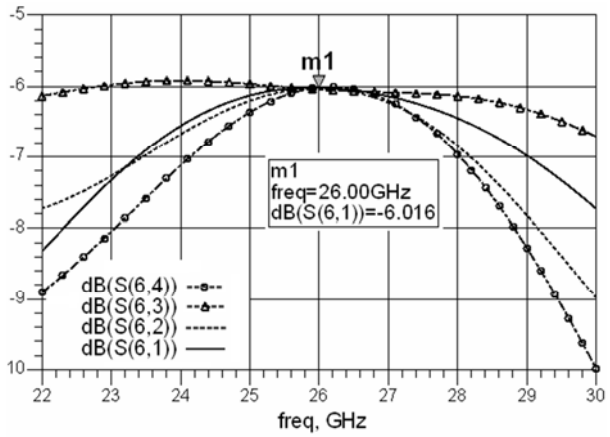

Fig. 12. Transmission coefficients between RF input port (N°6) and output ports.

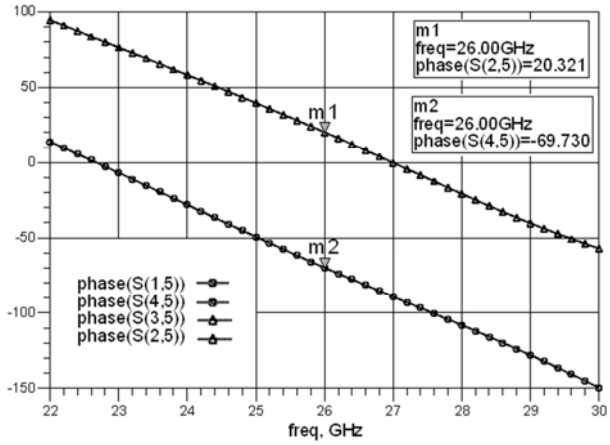

(a)

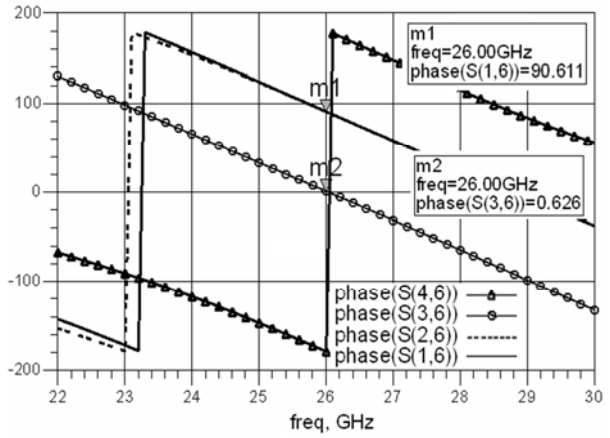

(b)

Fig. 13. Transmission phases: (a) S_{i5} , (b) S_{i6} with i = 1 to 4.

We can see that the phase difference is always around ± 90°.

All results obtained for the transmission coefficients and the transmission phases are consistent with the architecture of the modified six-port circuit represented in Fig. 6.

We finish this study par presenting the isolation curves as well for the two input ports as for the four output ports. Figure 14 shows that there is an excellent isolation between input ports 5 and 6 with about -36 dB at 26 GHz frequency.

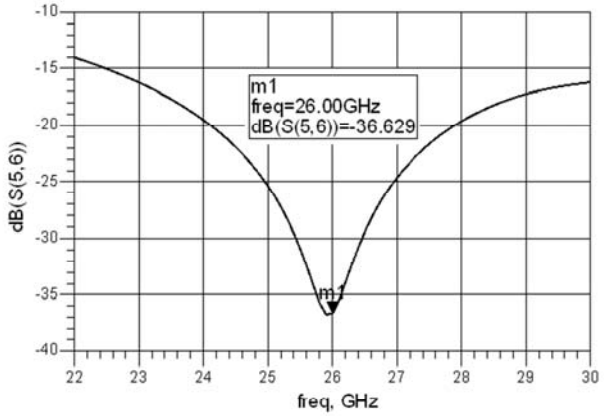

Fig. 14. Isolation (S_{56}) between input ports.

Figure 15 also shows that there is a good isolation between the output ports, all values being less than -33 dB at this frequency.

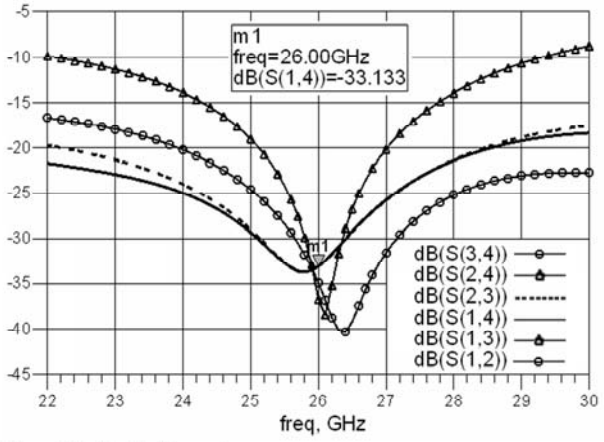

Fig. 15. Isolations between output ports.

V. ELECTROMAGNETIC SIMULATIONS OF THE SIX-PORT WITH A POWER DETECTION CIRCUIT

In order to take advantage of the qualities of the six-port circuit as a phase demodulator of a QPSK signal [11], we have made simulations based on some assumptions for the structure with the round hybrid couplers. To distinguish the four states of modulation, the output signals have to pass through a power detection circuit.

Figure 16 presents the diagram of the six-port circuit with a power detection circuit. Input ports 5 and 6 receive the reference signal from a local oscillator and the QPSK signal, respectively.

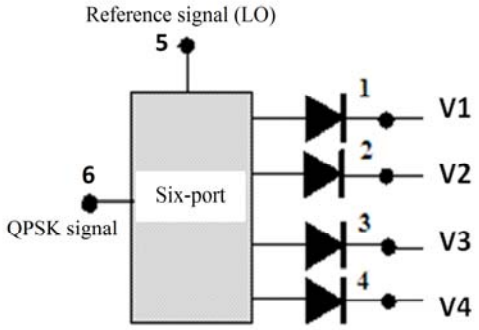

Fig. 16. The six-port with a power detection circuit.

DC voltage obtained at each output is proportional to the square of the amplitude of b_i [12]:

$$V_i = K_i \left| b_i \right|^2 . \tag{7}$$

The set of equations (8) shows that the power at each output depends on the phase difference between the input signals.

Assuming the detectors identical ($K_i = K$), we can write:

$$\begin{cases} V_1 = K\dfrac{|a|^2}{4}\left|1-\exp\left(j\Delta\theta\right)\right|^2 = K|a|^2\left|\sin\left(\dfrac{\Delta\theta}{2}\right)\right|^2 \\ V_2 = K\dfrac{|a|^2}{4}\left|1-\exp\left(j\left(\Delta\theta-\dfrac{\pi}{2}\right)\right)\right|^2 = K|a|^2\left|\sin\left(\dfrac{\Delta\theta-\dfrac{\pi}{2}}{2}\right)\right|^2 \\ V_3 = K\dfrac{|a|^2}{4}\left|1-\exp\left(j\left(\Delta\theta-\dfrac{\pi}{2}\right)\right)\right|^2 = K|a|^2\left|\sin\left(\dfrac{\Delta\theta-\pi}{2}\right)\right|^2 . \\ V_4 = K\dfrac{|a|^2}{4}\left|1-\exp\left(j\left(\Delta\theta-\dfrac{\pi}{2}\right)\right)\right|^2 = K|a|^2\left|\sin\left(\dfrac{\Delta\theta+\dfrac{\pi}{2}}{2}\right)\right|^2 \end{cases} \tag{8}$$

To obtain variations in amplitude of the output voltages relative to the phase shift between RF and reference signals, we vary the phase of the RF signal between 0° and 360° while maintaining constant the powers of the input signals, and the phase of the reference signal. Figure 17 shows the

variations of amplitudes V_1, V_2, V_3, and V_4 at ports 1, 2, 3, 4 depending on the phase shift between RF and LO inputs.

We can observe that every voltage has a single minimum or maximum value for a phase shift between reference and RF signals going from 0° to 360°. This phase shift can be determined using only the values of these voltages and relying on an appropriate algorithm.

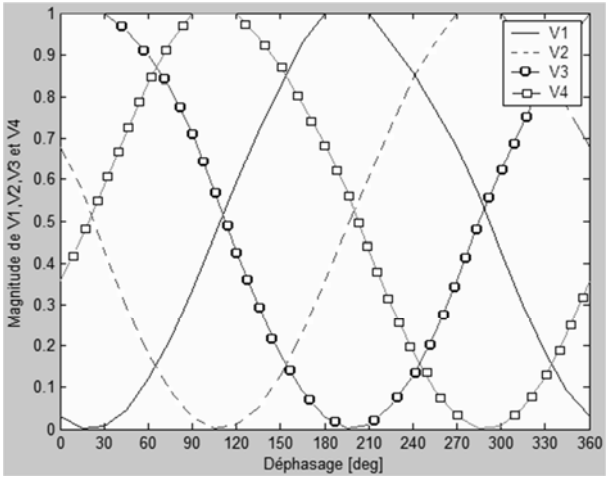

Fig. 17. Normalized output dc voltages versus the phase shift between RF and LO input signals.

The modified six-port circuit can then be regarded as a phase discriminator. In terms of phase shift between RF inputs, each function $V(\Delta\theta)$ is periodic with period 2π, and minimum values of the four voltages are separated by multiples of $\pi/2$. Subsequently, we can consider a method to obtain the constellation of the demodulated signal in the I/Q complex plane.

The phase θ_6 of the input signal contains the information while the phase θ_5 of the LO signal represents the reference. In the I/Q plane and using Eq. (9), we define a vector Γ representing a combination of the four dc output voltages [13].

$$\Gamma = \left[(V_3 - V_1) + j(V_4 - V_2)\right]\exp\left(j\frac{\pi}{4}\right). \qquad (9)$$

Figure 18 illustrates the four modulation states of a QPSK modulated signal.

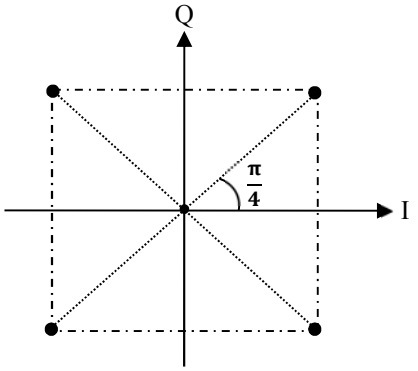

Fig. 18. QPSK modulation.

Assuming $\theta_6 = \frac{\pi}{4}$ with as reference $\theta_5 = \frac{\pi}{4}$, we obtain $\Delta\theta = 0$. Therefore, the output voltages can be expressed as follows:

$$V_1 = 0 \;\;\&\;\; V_2 = V_4 = \frac{1}{2}K|a|^2 \;\;\&\;\; V_3 = K|a|^2 \quad . (10)$$

So, the point obtained using Eq. (9) will be given by the vector $\Gamma = K|a|^2\exp\left(j\frac{\pi}{4}\right)$. This point is located in the center of the first quadrant of Fig. 18, which confirms that the signal is correctly demodulated.

Table 1 below presents the values V_1 to V_4 and Γ according to θ_6 and corresponding to the four modulation states.

Table 1: Theoretical demodulation results of a QPSK signal

θ_6	V_1	V_2	V_3	V_4	Γ
$\frac{\pi}{4}$	**0**	$\frac{1}{2}K\|a\|^2$	$K\|a\|^2$	$\frac{1}{2}K\|a\|^2$	$K\|a\|^2\exp\left(j\frac{\pi}{4}\right)$
$3\frac{\pi}{4}$	$\frac{1}{2}K\|a\|^2$	**0**	$\frac{1}{2}K\|a\|^2$	$K\|a\|^2$	$K\|a\|^2\exp\left(j\frac{3\pi}{4}\right)$
$5\frac{\pi}{4}$	$K\|a\|^2$	$\frac{1}{2}K\|a\|^2$	**0**	$\frac{1}{2}K\|a\|^2$	$K\|a\|^2\exp\left(j\frac{5\pi}{4}\right)$
$7\frac{\pi}{4}$	$\frac{1}{2}K\|a\|^2$	$K\|a\|^2$	$\frac{1}{2}K\|a\|^2$	**0**	$K\|a\|^2\exp\left(j\frac{7\pi}{4}\right)$

We can notice the excellent qualities of the modified six-port circuit as a phase demodulator. Thanks to this analytical development, we can confirm that with its new architecture, the six-port circuit can be suitably used as a phase demodulator of a QPSK modulated signal. Using the phase discriminator properties of the modified six-port circuit and an appropriate analog processing for the output signals, it becomes possible to demodulate other signals modulated in phase even though the circuit has been originally designed to demodulate a QPSK signal.

VI. CONCLUSION

The six-port junction was especially used for microwave instrumentation and measurements. The objective was to design a new microwave and millimeter wave direct conversion receiver based on a six-port frequency discriminator and dedicated to a high speed QPSK modulation. This junction was in the past designed and fabricated in monolithic hybrid microwave integrated circuit (MHMIC) and monolithic microwave integrated circuit (MMIC) with a certain complexity in manufacturing.

We propose in this paper a modified six-port circuit based on microstrip technology. It is distinguished by its simple and compact structure which allows an easy implementation of low cost and in addition provides a certain resistance to manufacturing imperfections. Note that there were no radiation problems in the functioning of this new structure which also has a high immunity to phase distortions and fluctuations in the power of the RF signal and adjacent channel.

Finally, we can assert that it is possible to realize a phase demodulator for an efficient QPSK modulated RF signal based on just a simple and compact structure.

ACKNOWLEDGMENT

The authors would like to thank Dr. J. Belhadj Tahar of Higher School of Communication of Tunis for his valuable contribution in this work. They would also like to acknowledge the constructive comments and suggestion provided by the reviewers. Their kind effort certainly contributed to the quality of this publication.

REFERENCES

[1] F. D. L. Peters, D. Hammou, S. O. Tatu, and T. A. Denidni, "Modified Millimeter-Wave Wilkinson Power Divider for Antenna Feeding Network," *Progress In Electromagnetics Research Letters*, vol. 17, pp. 11-18, 2010.

[2] N. Seman, M. E. Bialkowski, S. Z. Ibrahim, and A. A. Bakar, "Design of an Integrated Correlator for Application in Ultra Wideband Six-Port Transceivers," *IEEE Antennas and Propagation Society International Symp.*, pp. 1- 4, June 2009.

[3] M. Mohajer and A. Mohammadi, "A Novel Architecture for Six-Port Direct Conversion Receiver," *15th IEEE International Symposium on Personal, Indoor and Mobile Radio Communications*, vol. 4, pp. 2705-2709, Sept. 2004.

[4] V. Demir, D. Elsherbeni, D. Kajfez, and A. Z. Elsherbeni, "Efficient Wideband Power Divider for Planar Antenna Arrays," *Applied Computational Electromagnetics Society (ACES) Journal*, vol. 21, no. 3, pp. 318-324, Nov. 2006.

[5] A. Mohra, A. F. Sheta, and S. F. Mahmoud, "New Compact 3dB 0/180 Microstrip Coupler Configurations," *Applied Computational Electromagnetics Society (ACES) Journal*, vol. 19, no. 2, pp. 108-112, July 2004.

[6] G. F. Engen, "The Six-Port Reflectometer: An Alternative Network Analyzer," *IEEE Transactions on Microwave Theory and Techniques*, vol. 25, no. 12, pp. 1075-1080, Dec. 1977.

[7] S. Ibrahimpasic and M. Hasanovic, "Modeling and Simulation of Wilkinson Power Splitter in Suspended Stripline," *Applied Computational Electromagnetics Society (ACES) Journal*, vol. 25, no. 10, pp. 888-893, October 2010.

[8] A. S. Al-Zayed, Z. M. Hejazi, and A. S. Mohra, "A Microstrip Directional Coupler with Tight Coupling and Relatively Wideband Using Defected Ground Structure," *Applied Computational Electromagnetics Society Journal*, vol. 25, no. 10, pp. 877-887, October 2010.

[9] S. O. Tatu, K. Wu, and T. A. Dendini, "Direction of Arrival Estimation Method Based on Six-Port Technology," *IEE Proceedings - Microwaves Antennas and Propagation*, vol. 153, no. 3, pp. 263-269, June 2006.

[10] "Advanced Design System," 2005 [Online]. http://www.ece.uci.edu/eceware/ads_docs/

[11] I. Molina-Fernandez, J. G. Wanguemert-Perez, A. Ortega-Monux, R. G. Bosisio, and K. Wu, "Planar Lightwave Circuit Six-Port Technique for Optical Measurements and Characterizations," *Journal of Lightwave Technology*, vol. 23, no. 6, pp. 2148-2150, June 2005.

[12] D. Hammou, E. Moldovan, K. Wu, and S. O. Tatu, "60 GHz MHMIC Six-Port Model Analysis," *Microwave and Optical Technology Letters*, vol. 52, no. 9, Sep. 2010.

[13] G. Vinci, A. Koelpin, F. Barbon, and R. Weigel, "Six-Port-Based Direction-Of-Arrival Detection System," *Asia-Pacific Microwave Conference Proceedings (APMC)*, pp. 1817-1820, Dec. 2010.

Lotfi Osman received his Ph.D. degree in Automatic & Industrial Computing from the University of Lille 1, France, in 1987. He is currently Assistant Professor with the Department of Electronics, Physics and Propagation at the Higher School of Communication of Tunis, Sup'Com. In 2004, he joined the Research Unit "CSEHF" at the Faculty of Sciences of Tunis, Tunis El Manar University. His current research interests include antennas and modeling in microwave integrated circuits. He is also involved with experimental characterization and antenna measurement.

Imen Sfar was born in Tunis in 1978, she received in 2006 her master's degree in Electronics from the Faculty of Sciences of Tunis, Tunisia, where she's currently working toward her Ph.D. Her current research interests include antennas for wireless communication and analysis of microwave structures.

Ali Gharsallah Professor at the Faculty of Sciences of Tunis and Head of Research Unit "CSEHF" (code 05/UR/11-10) at the Department of Physics, Faculty of Sciences of Tunis, El Manar University. He received the engineering's degree in radio-electrical from the Higher School of Telecommunications of Tunis in 1986 and the Ph.D. degree in 1994 from the National Engineering School of Tunis. Since 1991, he was with the Department of Physics at the Faculty of Sciences of Tunis. His current research interests include antennas, multilayered structures and microwave integrated circuits.